Neuronal Patterns in the Cavity Wall of Lesions during Gait Cycle in a Rat Model of Brain Lesion Cavities

Ioana Nica[1], Marjolijn Deprez[2], Frederik Ceyssens[3], Kris van Kuyck[2], Robert Puers[3], Bart Nuttin[2,4]
and Jean-Marie Aerts[1]

[1]*Division Measure, Model & Manage Bioresponse (M3-BIORES), Department of Biosystems, KU Leuven, Leuven, Belgium*
[2]*Research Group Experimental Neurosurgery and Neuroanatomy, KU Leuven, Leuven, Belgium*
[3]*Division Microelectronics and Sensors(MICAS), Department of Electrical Engineering, KU Leuven, Leuven, Belgium*
[4]*Department of Neurosurgery, University Hospitals Leuven, Leuven, Belgium*

Keywords: Beta Oscillations, Frequency Modulations, Local Field Potential, Motor Cortex, Rehabilitation, Brain Lesion, Gait.

Abstract: Oscillatory neural activity was reported to have various physiological roles in information processing of brain functions. It is now established that extracellular activity in the motor cortex encodes aspects of movement, involving planning and motor control. Oscillatory patterns have also been hypothesized to play a role in brain recovery and functional remapping. In this study, we measured neural activity from within the cavity wall of a motor cortex lesion, in a rat model, while the animals performed a skilled walking task. We aim at providing a possible framework of analysis, focused on revealing oscillatory patterns in the cavity wall and their correlation with motor deficits, by using a combination of spectral features, involving power spectra and coherence estimates in the beta and gamma frequency bands.

1 INTRODUCTION

Synchronization phenomena have been shown to play a significant role in processing information in the nervous system, in the case of normal or pathological brain activity. Strongly synchronized oscillations occurring at the neuronal level can be identified in measurements performed at the population level, like local field potentials (LFPs).

Oscillations are reported to be related to the planning and generation of movements in healthy subjects. In a number of invasive and non-invasive studies, in humans and animal models, prominent 10-30 Hz beta oscillations have been observed in motor cortical and subcortical structures in idle subjects (Jasper et al., 1949; Toma et al. 2000; Neuper and Pfurtscheller, 2001; Alegre et al., 2002); beta oscillations tend to get suppressed when the subject begins planning a movement, while the 40-90 Hz gamma band oscillations emerge (Bouyer et al., 1981; Donogue et al., 1998; Hamada et al., 1999; Aoki F. et al., 2001). On the other hand, oscillations are also an expression of motor deficits. In

Parkinson's disease, increased synchronization in beta oscillations in the basal ganglia has been reported as probable underlying cause in manifestation of resting tremor, bradykinesia, and rigidity (Raz et al., 1996, 2000; Ruskin et al., 1999, 2003; Goldberg et al., 2004).

More recently, it has been hypothesized that synchrony might play a key role in triggering self-repair processes after brain injury. It is thought that spontaneous modulation of extracellular fields and emergence of synchronous activity act as a signal for axonal sprouting (Carmichael et al., 2002) and may influence Hebbian plasticity mechanisms, that favor rewiring of neural pathways (Murphy and Corbett, 2009).

In this study, we aimed at developing a methodology to quantify patterns of oscillatory neural activity within the wall of cortical lesions. The approach allows investigation of motor deficits in relation with continuous neural input in the region of lesions induced on the motor cortex of rats.

2 METHODS

We lesioned the contralateral forelimb area of the primary motor cortex (M1) in nine rats that have been trained to walk along a horizontal ladder with unequally spaced rungs. We examined gait cycle kinematics visible from video recordings of the rat performing the task, and spectral features of the simultaneously recorded LFPs.

The lesion caused a decrease in movement precision, grasping strength and crossing speed in the affected limb. However, the rats were still capable of movement planning and control. Oscillatory activity in electrophysiological signals can be captured with a wide range of time-frequency transforms. Since we recorded LFPs via a 4x4 multi-electrode array that spans over the wall of the lesion, we propose a space-time-frequency method of analysis. We focus on power and inter-electrode coherences in the beta and gamma bands, to investigate dynamical relationships between electric activity captured at the 16 electrode locations.

2.1 Animal Preparation and Surgical Techniques

Before training started, the animals (nine male Sprague-Dawley rats) were housed individually and put on a restricted feeding schedule until the body weight reduced with ± 10%. They were trained for four consecutive days to walk over the horizontal ladder in one direction. After training, a lesion was created by aspiration of the forelimb area in the primary motor cortex. The lesion was made in the contralateral hemisphere to the preferred limb (which was determined using the pasta matrix reaching task). Lesions were made at the following coordinates: 5 mm anterior to 1 mm posterior to bregma, and 0.5 to 4.5 mm lateral to bregma. The rats were allowed to recover for 3 weeks after which the electrode array (Fig.1.a) was implanted against the lesion cavity wall. After implantation, the lesion cavity was filled with medical silicone (Kwik-Sil) to keep the electrode array in place. Arrays were implanted against the center and posterior cavity wall, since the array was not large enough to cover the entire lesion cavity wall (this placement was determined based on the first rat, where it was not possible to implant the electrode against the anterior wall). The implant was secured with screws and dental cement (Fig.1.b). Electrode arrays were produced in house by the Electrotechnical Engineering department (MICAS-ESAT) of the KU Leuven. They consisted of 16 Platinum contacts each with a diameter of 350 µm. Electrode contacts were spaced ± 1.3 mm apart from each other.

a.   b.   c.
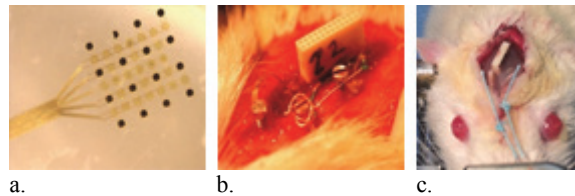
Figure 1: a. electrode array; b. view of the lesion site after electrode and connector implantation; c. top view of the rat head with headstage and connector.

2.2 Experimental Setup and Recordings

Two weeks after electrode implantation, the animals motor ability was tested by performing the horizontal ladder walking they were trained for. We performed three trials per rat, during which LFP and video recordings were performed simultaneously.

Video recordings were taken at a sampling rate of 40Hz with an iDS GigE camera (iDS Imaging Development Systems GmbH, Obersulm, Germany). To check for lost video frames, a LED flashing protocol was implemented, so that a bursting flash could be visible on the upper part of the frame at a predetermined rate. Based on this, we implemented a custom automatic video tracking algorithm in Matlab to detect the flashes and synchronize camera frames with LFP timestamps.

LFP recordings were performed at a sampling rate of 10 kHz, wirelessly, using the W16 model from Multichannel Systems (MCS GmbH, Reutlingen, Germany), placed on top of the rat's head (Fig.2). The electrodes were connected to the headstage via an Omnetics connector (npd-18-VV-GS). The LFPs were preamplified in the range of 1Hz to 5 kHz and digitized within the headstage, before the transfer to the receiver.

a.   b.
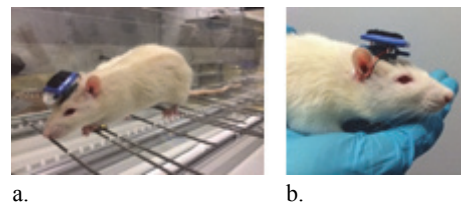
Figure 2: a. side view during the ladder test;   b. view of the headstage location.

2.3 Data Processing

The data processing was performed in Matlab, version 2013b, using the available toolboxes and custom algorithms.

2.3.1 Behaviour Labelling

The video recordings were analysed frame by frame, to identify and describe quantitatively components of the rat gait cycle according to a scoring system presented elsewhere (Metz and Whishaw, 2009). Extracted features are summarized in Table 1.

The initial group consisted of a number of 20 rats, 6 of which died before the experiment was concluded. Based on the video analysis, 5 more rats were excluded, since the high number of stops and long delays while crossing the ladder would not allow for a significant number of consecutive completed gait cycles to be analysed. Three trials per rat were analysed, the results presented in Table 1 represent the mean over all movements identified in the three trials.

We analysed general features like latency (time needed to cross the ladder) and number of times the rat stops while being on the ladder, but also quantitative features related to the accuracy of foot placement and forepaw dexterity (according to (Metz and Whishaw, 2009)).

Limb placement was scored on a scale from 0 to 6, and the individual scores were defined as follows: midportion of the palm of the limb is placed on the rung with full weight support (6 points); the limb is partially placed on the rung with either wrist or digits of the forelimb or heel or toes of a hind limb (5 points); the limb aims for one rung but it is placed on another rung without touching the first one or, alternatively, the limb is placed on a rung but quickly repositioned (4 points); the limb is placed on

a rung, but before it bears the weight, it is repositioned on another rung (3 points); the limb is placed on a rung, slips off slightly during weight bearing without disrupting the gait cycle (2 points); the limb is placed on the rung and slips off when weight bearing which leads to a fall (1 point); the limb completely misses the rung and falls (0 points). We analysed the movement of all four limbs: left and right forelimbs (LFl, RFl) and left and right hind-limbs (LHl, RHl).

Out of these, only the slips (score of 0-3) were considered errors of foot placement.

Accuracy of forepaw placement and ability to grasp were also considered, using a four-category scale, as follows: digits completely flexed around the rung (3 points), digits flexed in a 45˚ angle (2 points), digits placed in a 90˚ angle on the rung (1 point); forepaw partially placed on the rung, with either wrist or tips of digits resulting in no grasp (0 points).

These scores provide an indication regarding the position of the lesion and the functional area affected; for instance, in some rats, the lesion equally affects the contralateral fore- and the hind-limbs.

2.3.2 LFP Analysis

We are interested in capturing oscillatory events and synchrony, therefore, we focused on spectral features of the local field potentials.

LFPs were down-pass filtered with a cut-off frequency of 300 Hz (elliptic filter with passband ripple of 0.5 dB and stopband attenuation of 60dB). Since the recordings were performed wirelessly, no powerline interference was visible and the data was artefact-free.

Based on the video analysis, intervals of gait cycles were identified and included in the analysis,

Table 1. Features used in scoring rat kinematics.

Rat (impaired limb)	Latency (sec)	Total number of stops	Limb fault scoring (0 - 6)				Number of slips (Fl/Hl)		Forepaw digit score (0 - 3)	
			LFl	RFl	LHl	RHl	Left	Right	LFl	RFl
2 (RFl)	9.57	6	5.1	5	5.8	4.7	0/1	2/4	1.3	1
9 (RFl)	11.9	5	5.3	5.7	5.2	5.5	2/2	0/1	0.9	1.8
11 (RFl)	8.93	5	5.6	5.4	5.2	3.9	0/3	3/6	1.6	1.6
4 (LFl)	8.07	2	5.2	5.8	4.7	5.6	1/2	0/0	0.8	1.4
6 (LFl)	9.6	0	4.6	5.3	4.6	4.8	4/3	0/3	0.9	0.9
8 (LFl)	9.64	4	5	5.2	5	4.6	2/2	0/3	0.5	0.7
10 (LFl)	9.54	6	4.9	5.8	5.8	5.4	1/3	0/0	0.8	1.3
13 (LFl)	10.2	4	4.8	4.7	4.7	5	4/3	2/2	1.4	1.5
14 (LFl)	9.17	6	5.3	5.7	5.6	5.1	0/0	0/2	1.6	1.5

(only intervals comprising of consecutive steps were taken into consideration, moments when the rat stopped were excluded).

We estimated coherence between the 16 channel recordings. Coherence - or, equivalently, magnitude-squared coherence ($C_{x,y}$) - provides a statistical measure of the similarity between signals at a given frequency and is defined in terms of the cross-spectral density of two signals x(t) and y(t) (G_{xy}), and normalized by their autospectra (G_{xx}, G_{yy}) as follows:

$$C_{x,y} = \frac{|G_{x,y}|^2}{G_{xx} G_{yy}} \quad (1)$$

Magnitude-squared coherence estimates were performed in Matlab, on epochs of approximately 250 msec (LFPs and video recordings were synchronized and the interval between 10 consecutive video frames was included in the coherence calculations) by taking a window of 50 msec, with 80% overlap.

a.

b.

c.
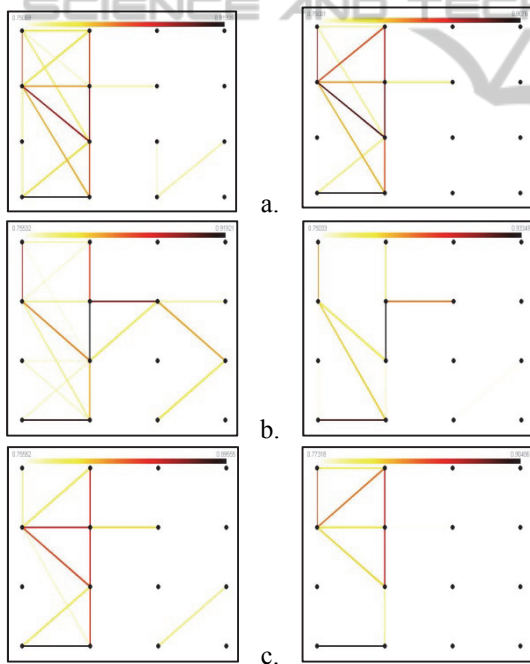
Figure 3: Example of patterns of coherences in the beta band on 100 msec epoch prior to (left column) and immediately after (right column) movement initiation. The coherence patterns were generated based on averages of at least 8 steps from the gait cycle of rat 2 such that in Figure 3.a.: epochs were selected for good steps; in Figure 3.b.: epochs were selected for under-reached steps; in Figure 3.c.: epochs were selected for over-reached steps. The orientation of the maps with respect to global coordinates is North - anterior, South - posterior.

Coherence values were calculated for 120 possible pairs between the 16 electrodes, for frequencies below 250 Hz. The resulting values were averaged for the intervals of 15-30 Hz (beta band), 30-45 Hz (low gamma) and 45-90 Hz (high gamma).

Only coherence values beyond a threshold, consisting of 125% of the mean over the 250 msec epoch were taken into consideration and further organized in a 16x16 adjacency matrix, used to generate an undirected graph, that can be interpreted as a map of significant coherences at a certain frequency band (see Fig. 3).

$$A(G)_{ij} = \begin{cases} 1, if\ i = j \\ 0, otherwise \end{cases} \quad (2)$$

The vertices represent electrode locations and the edges connecting them indicate the strength of the coherence, according to the colormaps. This way of estimating coherences over short time-windows can be used to interpret data on-line, and it was implemented so as to match the sampling rate of the video, as a way of visualizing behavior and neural activity simultaneously. It incorporates information about frequency, time localization and spatial location of most active connected sites within the lesion in a bi-dimensional form.

3 RESULTS AND DISCUSSION

Based on preliminary analysis, our hypotheses are as follows: (i) coherence maps could be used to better understand the nature of an individual's deficit, by using as feature the location of the 'maximally connected' electrode locations (these are vertices with maximum number of significant coherence pairs); (ii) the quality of a gait cycle could be quantified and predicted, by determining the structure of a specific coherence map per individual rat, on a preliminary training set of steps (with features such as the location of the significant coherence pairs and their strength); (iii) a possible feature in detecting movement onset could be the number of significant coherence pairs (out of a maximum of 120) between the 16 electrode contacts.

In Figure 4, a representative example for the power content of the signals during one ladder run is provided: as observed, the lower, 10-Hz frequency power is consistently high and non-discriminative, while there is a continuous power shift between beta and the higher gamma-band, which was not observed to be directly correlated to the movement

onset, gait pattern or the specific type of errors in movement coordination. However, it is this power shift in power content in the higher frequency bands that motivated the choice for beta and gamma bands in the coherence investigation.

The behavior analysis revealed the deficit of some rats to be more extensive than expected. For instance, in Rat 2, the higher deficit is apparent in the hind-limb. Therefore, in the corresponding coherence maps illustrated in Figure 3, we expect the region in the lower half to be also active, to account for the involvement of the hind limb functional area of the motor cortex and as shown, the pattern is indeed concentrated in the left side of the map. However, the main challenge in interpreting these results is related to the question of how observable the system is from our recordings, since there is a strict dependence on the placement of the electrode array within the lesion.

Regarding the second hypothesis, a recurrent observation is that on correct steps, there is a focalized center of coherence, whereas on the onset of an erroneous step, the connections are more dispersed.

However, we investigated a very limited number of examples from individual rats, a validation would require an extensive longitudinal study.

The third hypothesis is sustained by the observation that, on movement onset, the number of significant beta coherences decreases, while the number of gamma coherences increases, where a significant level was defined as the value at least equal to 125% of the mean coherence over all coherence maps calculated within one ladder run. An example is provided in Figure 5, where the average number of significant coherence pairs is approximated on a window equivalent to the interval spanned by 10 video frames. This feature is then plotted against time, for the course of a ladder run. The vertical lines indicate the intervals of swing on the affected limb (left fore-limb, in the example provided, for rat 6). To be noted is that all the other limbs are moving as part of a normal gait cycle sequence. An interesting question would be whether or not there exists a feature discriminating initiation of swing on each limb, or if there is a rather more global biomarker, specific to the initiation of gait. In order to test this idea, the resting state condition should be included in the experiment.
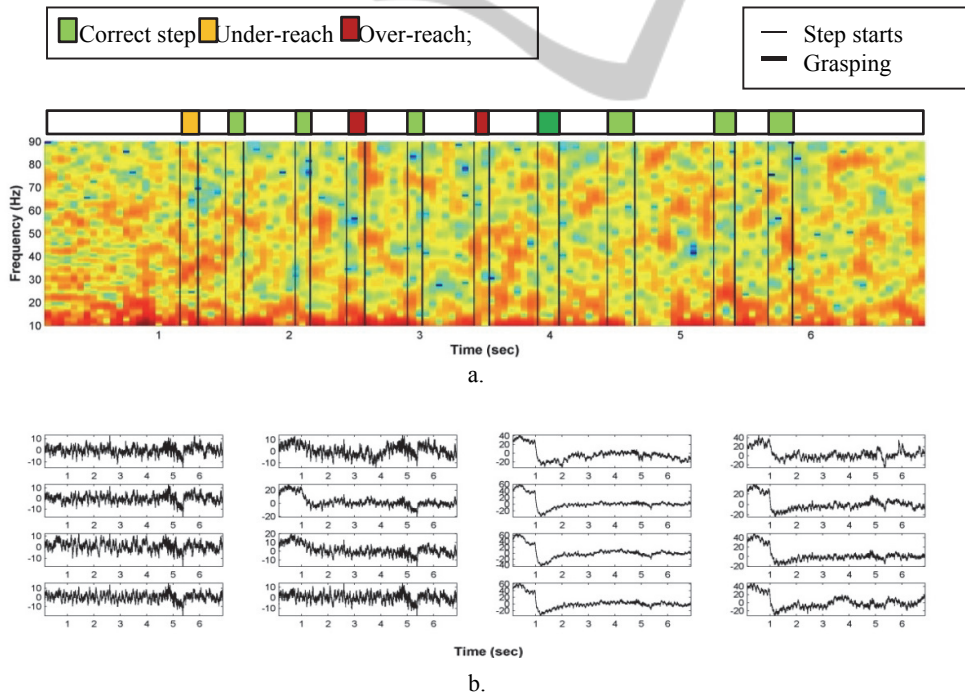
Figure 4: Example of power content and signal waveform for the 4x4 electrode array during one ladder run. Figure 4.a.: mean power spectra content of the 16 LFP channels in the 10-90 Hz band during one ladder run (from rat 4, swing intervals identified for the left forelimb; power spectrum calculated on windows of 20 msec, with 80% overlap); the intervals of gait swing and the labels for each step are provided according to the color code. Figure 4.b.: Corresponding LFP traces from the 16 channels.
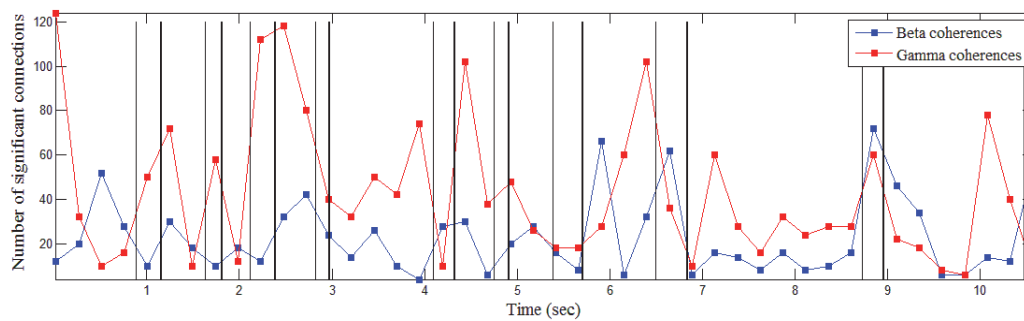
Figure 5: Variation of number of connections during a ladder run test.

4 CONCLUSIONS AND FUTURE WORK

In order to characterise motor deficits in a rat model of brain lesion cavities, we developed a methodology involving behaviour analysis along with investigation of local field potentials originating from the cavity wall of the cortical lesion.

Based on preliminary results, coherence measures of the neural activity within the cavity wall may prove valid in discribing the nature of the functional deficit, but also, the configuration of coherence maps may constitute signatures for movement initiation and coordination. An immediate objective would be to design a more extensive cross- and longitudinal study, to test the two hypotheses.

The method we propose for generating coherence maps cand be easily implemented in an on-line configuration, to characterise signal similarity in three dimensions: frequency, space and time.

REFERENCES

Aoki, F., et al., 2001. Changes in power and coherence of brain activity in human sensorimotor cortex during performance of visuomotor tasks.

Alegre, M., et al., 2002. Beta electroencephalograph changes during passive movements: sensory afferences contribute to beta event-related desynchronization in humans. *Neurosci. Lett.*, 331, 29.

Donogue J.P. et al., 1998.Neural discharge and local field potential oscillations in primate motor cortex during voluntary movements, *J. Neurophysiol.,* 79, 159.

Goldberg JA, Rokni U, Boraud T, Vaadia E, Bergman H (2004) Spike synchronization in the cortex-basal ganglia networks of parkinsonian primates reflects global dynamics of the local field potentials. *J Neurosci* 24: 6003-6010.

Hamada, Y., Miyashita, E., and Tanaka, H., 1999. Gamma-band oscillations in the 'barel cortex' preced rat's exploratory whisking. *Neuroscience*, 88, 667.

Jasper, H., and Penfield, W., 1949. Electrocorticograms in man: effect of voluntary movement upon the electrical activity of the precentral gyrus, *Arch. Psychiatrie und Z. Neurologie*, 182, 163.

Metz, G.A., Whishaw, I.Q., 2009. The ladder rung walking task: a scoring system and its practical application. *J. Vis. Exp.* (28), e1204, doi:10.3791/1204.

Murphy, T. H., and Corbett, D., 2009. Plasticity during stroke recovery: from synapse to behaviour. *Nat. Rev. Neurosci.* 10, 861–872.

Neuper, C., and Pfurtscheller, G., 2001. Evidence for distinct beta resonance frequencies in human EEG related to specific sensorimotor cortical areas. *Clin. Neurophysiol.,* 112, 2084.

Raz, A., Feingold A., Zelanskaya V, Vaadia E, Bergman H (1996) Neuronal synchronization of tonically active neurons in the striatum of normal and parkinsonian primates. *J Neurophysiol* 76: 2083-2088.

Raz A, Vaadia E, Bergman H (2000) Firing patterns and correlations of spontaneous discharge of pallidal neurons in the normal and the tremulous 1-methyl-4-phenyl-1,2,3,6-tetrahydropyridine vervet model of parkinsonism. *J Neurosci* 20: 8559-8571.

Ruskin DN, Bergstrom DA, Kaneoke Y, Patel BN, Twery MJ, Walters JR (1999a) Multisecond oscillations in firing rate in the basal ganglia: robust modulation by dopamine receptor activation and anesthesia. *J Neurophysiol* 81:2046-2055.

Toma, K., et al., 2000. Desynchronization and synchronization of central 20-Hz rhythms associated with voluntary muscle relaxation: a magnetoencephalographic study. *Exp. Brain Res.,* 134, 417.